Delft University of Technology

First order multi-lane traffic flow model – an incentive based macroscopic model to represent lane change dynamics

Nagalur Subraveti, Hari; Knoop, Victor; van Arem, Bart

Important note
To cite this publication, please use the final published version (if applicable).
Please check the document version above.

Taylor & Francis
Taylor & Francis Group

Check for updates

First order multi-lane traffic flow model – an incentive based macroscopic model to represent lane change dynamics

Hari Hara Sharan Nagalur Subraveti, Victor L. Knoop and Bart van Arem

Department of Transport and Planning, Faculty of Civil Engineering and Geosciences, Delft University of Technology, Delft, Netherlands

ABSTRACT

Unbalanced lane usage on motorways might lead to the reduction in capacity of the motorway. Lane-level traffic management present new opportunities to balance the lane-flow distribution and help reduce congestion. In order to come up with efficient traffic management strategies on a lane-level, there is a need for accurate lane-specific traffic state estimation models. This paper presents a first-order lane-level traffic flow model. The proposed model differs from the existing models in the following areas: (i) incentive-based motivation for lane changes and consideration of downstream conditions (ii) transfer of lateral flows among cells. The model is tested against real-world data. It is observed that the model is able to capture the lane-level dynamics in terms of the lane flow distribution. The model results are compared to a linear regression model and results show that the developed model performs better than the regression model on the test sections.

Introduction

Congestion on motorways has become a common phenomenon across the world and causes major discomfort to the road users and high societal costs. In order to come up with efficient and active traffic management strategies to tackle the problem of congestion, accurate modelling and prediction of traffic conditions are essential. Most of the existing real-time estimation and prediction methods aggregate traffic across lanes without taking into account the difference among lanes. But it has been observed that on multi-lane motorways, lanes operate differently. Depending upon the conditions, proportion of flows on different lanes vary (Duret, Ahn, and Buisson 2012; Knoop et al. 2010; Wu 2006). This can lead to underutilization of multi-lane motorways, with the possibility of congestion setting in on heavily used lanes even though spare capacity is still available on other lanes. In case of right hand traffic, the majority of the traffic is using the right most lane at very low densities. With increase in the roadway density, drivers start using the other lanes with the median lane being used the most at very high densities. Hence, knowledge of lane specific traffic conditions are important to achieve a more balanced distribution of traffic across the lanes and improve the efficiency of motorways. For effective lane-level traffic control, model based estimation and prediction frameworks are essential which can compute traffic flows on multi-lane motorways including the dynamics of lane changing.

This paper introduces a first order multilane traffic flow model that can represent the important lane changing dynamics. The proposed model differs from the existing models in the following areas: (i) computation and transfer of longitudinal and lateral flows (ii) incentive based motivation for lane

---

CONTACT Hari Hara Sharan Nagalur Subraveti ✉ h.h.s.nagalursubraveti@tudelft.nl

changes and consideration of the downstream conditions. Lane change rates are computed as a function of various incentives such as maintaining route, keep-right bias, changing to lower density lanes, etc. Incentives are formulated in such a way that no new parameters are introduced and the parsimonious representation of the earlier models is maintained. The model is then tested for a homogenous stretch and a lane drop section. The results of the model are then compared to a linear regression model.

The remainder of the paper is organized as follows: Section 2 describes state-of-the-art on multi-lane traffic flow models. Section 3 describes the proposed multilane traffic flow model including the computation and transfer of lateral flows and lane change rates based on incentives. In Section 4, the proposed model is calibrated and validated against real world data from two motorway sections. In Section 5, discussions on the results of the model and sensitivity of the model to parameters are reported, and finally in Section 6, we conclude the paper and mention recommendations for future works.

State-of-the-art on multi-lane traffic

Although motorway lane changing has gained significant attention in the last two decades, most of the research has been in the microscopic direction where lane changing decisions of individual drivers are evaluated and considered to be a function of multiple variables such as speed and positions of surrounding vehicles, gaps, road geometries etc. (Gipps 1986; Toledo, Koutsopoulos, and Ben-Akiva 2003; Kesting, Treiber, and Helbing 2007). Microscopic models require detailed vehicle information which might be difficult to collect. These models also usually consist of a large number of parameters which can be quite difficult to estimate and calibrate. Hence, employing the use of microscopic models for real time traffic state evaluation of multi-lane motorways seems unrealistic.

Macroscopic models describe aggregate driving behaviour and typically involve a relationship between the density and flow of a network. One of the earliest works related to multi-lane modelling from a macroscopic perspective was by Munjal and Pipes (1971) which was an extension of the kinematic wave model for a two-lane highway. Michalopoulos, Beskos, and Yamauchi (1984) improved upon this work and developed a second order model considering the acceleration effects and extended it to highways with more than two lanes. These models however were formulated in a continuous space–time domain and could not be applied successfully due to the lack of numerical schemes for discretization at that time. Laval and Daganzo (2006) expanded on the earlier works and presented a hybrid model considering the lane changers as particles with bounded acceleration rates. The main incentive considered here for drivers to change lane is to increase their speed. A major drawback of these models is that they consider the traffic flow variables to be aggregated across lanes which is not the case. Shiomi et al. (2015) and Roncoli, Papageorgiou, and Papamichail (2015) presented first order multi-lane models considering the lane changing rates to be dependent upon speed difference and density difference of neighbouring lanes respectively. These models treated the lanes as independent entities and did not aggregate the variables. Pan et al. (2016, 2019) proposed a mesoscopic multilane model to capture the multilane traffic dynamics and extended it to include multiclass mixed traffic of Connected and Automated Vehicles (CAV) and regular vehicles. The mesoscopic model requires the calibration of a number of parameters along with the fundamental diagram (FD) parameters. Jin (2010; Jin and Laval 2018) introduced a new variable called the lane-change intensity which affects the speed-density relationship and developed a macroscopic multi-lane model and recently proposed a unified model which integrated the bounded acceleration concept of Laval and Daganzo (2006).

A major element of most of the existing models is the calculation of lane change rates and transfer of lateral flow among cell segments in the discretization scheme. The transfer of lateral flow among cell segments in different lanes is considered to be diagonal, i.e. the lateral flow from a cell depends on the supply capacity of the adjacent downstream cell. While this works in the free-flow state, it may not work in congested conditions where the lateral demand is generally dependent on the receiving

capacity of both the adjacent cell and downstream cell in the target lane (especially when the length of the cell segments are not too long). Considering a diagonal transfer of flow among cell segments can lead to the under-estimation of the distance over which the congestion propagates as well as the erroneous estimation of the strength of congestion.

Existing literature consider either the speed difference or density difference between cells on adjacent lanes as an incentive to compute the percentage of flow that might change lane. But such a simple motivation cannot represent many cases such as lane drops and other mandatory manoeuvres where vehicles need to change lane irrespective of lower speed/higher density on the adjacent lane. Also, the keep-right behaviour generally observed in Europe and many other countries is generally neglected in most models (with the exception of Shiomi et al.) which again leads to inaccurate estimation of state variables. Seraj, Bie, and Qiu (2017) incorporated microscopic lane-changing theory within their macroscopic model and considered both speed and density differences as reasons for lane changing. Although the model was able to reproduce satisfactory lane changing patterns, this approach led to more number of parameters being introduced increasing the cost of calibration while not massively improving accuracy. Park et al. (2015) considered the influence of both speed and density difference in a log-regression model to explain discretionary lane changes in a mesoscopic scale. Laval and Daganzo (2006) used speed difference as motivations for lane change but it was based on the assumption of similar operating speeds across lanes which is not the case. Shiomi et al. (2015) also considered speed difference as motivation but took into account the different speeds across lanes (different FD for every lane). A single FD for all lanes implies that lane changes always happen among the lanes which is not the case (because of different operating speeds on each lane). The overtaking behaviour is also restricted by a keep-right bias. Hence, using a single FD for all the lanes might not lead to accurate results. Assuming the use of a triangular FD, one of the disadvantages of using speed as a motivation to explain lane changing is the constant relationship between speed and density in the free-flow state. This implies that no lane changes take place in the free flow state which is not a realistic assumption. Considering different shapes of FD to allow for lane changes in the free-flow state can increase the complexity of the model in terms of the computation of demand and supply capacities due to the introduction of nonlinear terms. Hence, relation between the densities on different lanes offers more opportunities for the computation of lane change rates even in free-flow conditions.

In this study, the motivation behind lane changing is formulated more explicitly using different incentives related to the densities of lanes rather than speed to consider various types of lane changing scenarios. The transfer of lateral flows is also based on the assumption that the lateral demand is dependent upon the supply capacity of the adjacent and downstream cell segments on the target lane to yield more accurate results. The developed model is tested against real world data. The results are then compared to a benchmark model which is also not commonly found in the existing literature.

First order multi-lane traffic flow model

Modelling framework based on CTM

Similar to most first order models, the starting point of the model is the well-known CTM (Cell Transmission Model) by Daganzo (1994) which is extended suitably to consider the dynamics of lane changing. A multi-lane motorway subdivided into segments, wherein each segment comprises of a number of lanes is considered. The segments are indexed $i = 1,2,3 \ldots .n$ and the lanes as $l = 1,2 \ldots .m$.

The conservation law of multi-lane traffic is given by (1) which has also been used in Munjal and Pipes (1971) and Laval and Daganzo (2006).

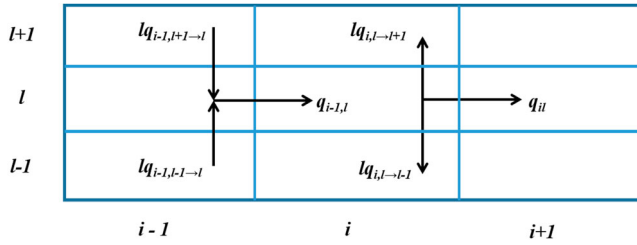$$\frac{\partial k_l(t,x)}{\partial t} + \frac{\partial q_l(t,x)}{\partial x} = \varphi_l, \quad l = 1,2,.,m \tag{1}$$

Figure 1. Representation of the discretized freeway.

$$\varphi_l = \sum_{l' \neq l} \varphi_{l' \to l} - \sum_{l' \neq l} \varphi_{l \to l'}$$

where, $\varphi_{l' \to l}$ is the lane change rate from lane l' to lane l. Using the notations from Figure 1 and based on the Godunov scheme of discretization for (1), the conservation equation in discrete terms is given by:

$$k_{il}(t+1) = k_{il}(t) + \frac{\Delta t}{\Delta x} * \left[q_{i-1,l}(t) - q_{il}(t) + lq_{i,l-1 \to l}(t) + lq_{i,l+1 \to l}(t) - lq_{i,l \to l-1}(t) - lq_{i,l \to l+1}(t) \right]$$
(2)

In (2), k and q represent the density and flow at the boundary of the cell-segments respectively. Δt is the size of the time step and Δx is the length of the cell segment. lq denotes the lateral flow between the cell segments. t denotes the simulation horizon where $t = 1,2,3 \ldots,T$ and the total simulation time is given as $t_{sim} = T * \Delta t$. In order to ensure numerical stability based on the Courant–Friedrichs-Lewy condition (CFL), the cell length must obey the following condition:

$$\Delta x \geq \max_{\forall l}(u_f) * \Delta t$$
(3)

where, u_f is the lane based free flow speed. To minimize the numerical diffusion, the length of the cell segments is chosen according to (4) which maps the length to the least integer greater than or equal to Δx.

$$\Delta x = \max_{\forall l}(u_f) * \Delta t$$
(4)

Computation of lateral flows

Generally, transfer of lateral flow from one cell can either be to the downstream cell in the target lane or to the neighbouring cell in the target lane as shown in Figure 2.

In the case of diagonal transfer, lateral flow depends upon the supply of the downstream cell in the adjacent lane. Although this is fine in free-flow conditions, it may not work in congested conditions. If the lane change rates are dependent only upon the supply of the adjacent downstream cell,
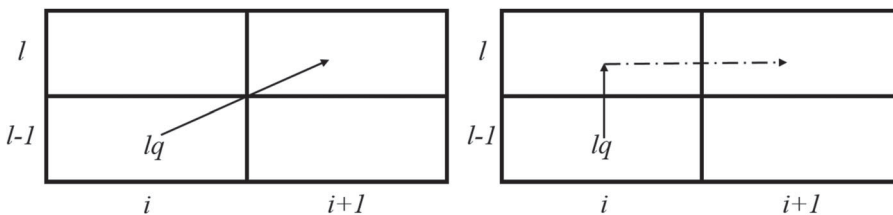

Figure 2. Transfer of lateral flow among cells.

the distance over which congestion propagates and its strength are incorrectly estimated. Hence, it is assumed that the lateral flow between lanes depends not only on the downstream cell of the adjacent lane but also on the adjacent cell of the target lane. So, a two-step model is proposed where initially, lateral demand and supply are calculated considering the supply capacity of the adjacent cells and then the longitudinal flows obtained from the previous step are transferred. In free-flow conditions, the proposed two step lateral flow transfer is similar to the diagonal flow transfer.

As has been previously highlighted in state-of-the-art, it is better to represent the lane change rates as a function of density difference among lanes as opposed to the speed difference. The advantage of using density difference is the fact that densities are the state variables of the traffic flow model being calculated and lane changes can occur even in free-flow conditions which is more realistic. Roncoli, Papageorgiou, and Papamichail (2015) used density difference as a motivation to explain lane changes. In this study, a term called the attractiveness rate was defined which was used to compute the lateral flow demand. It is given by:

$$A_{il \to l'}(k) = \mu * \max \left[0, \frac{P_{il \to l'} k_{il}(t) - k_{il'}(t)}{P_{il \to l'} k_{il}(t) + k_{il'}(t)} \right] \tag{5}$$

where μ and $P_{il \to l'}$ are parameters ranging from 0 to 1 reflecting the aggressiveness and location. For simplicity, $P_{il \to l'}$ was always taken as 1. While it has been mentioned that by varying the value of μ and $P_{il \to l'}$ for different locations and road configurations, the model can reproduce satisfactory results, a detailed explanation has not been provided by the authors. While (5) works for discretionary lane changes where the motivation to change lane is to improve the current situation, it can lead to inaccurate results in the case of mandatory lane changes where density difference is not of importance which places the importance on robust calibration of the location parameter $P_{il \to l'}$ in (5).

One of the factors that has rarely been considered in multi-lane models is the influence of downstream conditions on the computation of lateral flows. Unlike second order models which include the anticipative effect on speed, first order models do not have this advantage. There may be cases where the model predicts a lane change towards a lane considering lower density but a lane change may not be realistic. This problem has been highlighted in Shiomi et al. (2015) where drivers change lane from the middle lane to the median lane which is dropping. These kind of problems can be avoided by taking into account the downstream conditions. When downstream conditions are not considered, it can also result in lane hopping where vehicles continuously change to lower density lanes which is not realistic.

Considering the above highlighted limitations and requirements of the model, percentage of flow changing lanes in this model is taken as a function of the density difference among lanes similar to Roncoli, Papageorgiou, and Papamichail (2015) and is given by:

$$P_{il \to l'} = \max \left[0, \frac{IK_{il} - K_{il'}}{K_{il} + K_{il'}} \right] \tag{6}$$

The term I is considered to be a function of various incentives such as the density difference ($I_{\Delta k}$), route (I_r), keep-right bias (I_{kr}) and courtesy (I_{coop}) similar to the incentive based microscopic lane change model by Schakel, Knoop, and Van Arem (2012).

$$I = I_{\Delta k} + I_r + I_{kr} + I_{coop} \tag{7}$$

The different parts of I will be discussed in the forthcoming sections. The incentives are designed for smaller cell segment size and may not work well when the cell segments are too long (in the order of 1 km). In order to consider the effect of downstream conditions, the density term k in (5) is also replaced by a weighted density term K in (6) which is the weighted average of the considered cell segment and two downstream cell segments on the same lane. In the general case where there are no structural discontinuities, the value of I is equal to 1 implying the tendency to change lanes with lower density.

There are many reasons behind the lane change decision making and these reasons vary with road geometry, traffic conditions, vehicle type, etc. By including a multitude of parameters to explain lane changing, the advantage of parsimony that macroscopic models possess is nullified.

Keep-right incentive/(Lane change restriction incentive)

The term $I_{\Delta k}$ is considered equal to one in cases where the desire to change lane is only to improve the current condition. On a homogenous motorway stretch with no infrastructural bottlenecks in the vicinity, lane changes can mainly be attributed to the desire to move to a lane with higher speed or lower density. Since (6) has been formulated considering density, we will stick with the desire to move to a lower density lane. According to (6), any difference between the densities of cell-lane segments leads to lateral flow transfer. Although (6) eventually leads to lane flow equilibrium, continuous fluctuations in the intermediate sections leads to incorrect estimation of densities across lanes. Hence, it is required to censor lane changes and also take into consideration the keep-right behaviour generally observed on European motorways (keep-left in certain countries). According to this, vehicles are prohibited from overtaking to the right and stick to the right-most lane unless overtaking. Based on this argument, the incentive I_{kr} is formulated. It is argued that in free-flow conditions, vehicles change lane to the left only when the target lane is of sufficiently low density compared to their current lane and remain on their original lane for a certain threshold of density difference. The assumption is that if the density difference between the two lanes is quite low, drivers tend to stick to the right lane. So, in free-flow conditions, the term I_{kr} is given by:

$$I_{kr} = -\frac{k_{l'}}{k_l} \tag{8}$$

Using (8) in (7), the incentive to change lanes in free-flow conditions assuming other incentives are not active is:

$$I = 1 - \frac{k_{l'}}{k_l} \tag{9}$$

Since the incentive is formulated to restrict lane changes from right to left, (8) is valid only when $l' < 1$ (assuming lanes are numbered in ascending order from left to right). As can be seen from Figure 3, the range of density differences over which lane changes occur is greatly reduced. Thus, by including the term (8) in the computation of the lateral flow transfer, more realistic lane change rates towards the left can be expected. In congested conditions, lane changes are not restricted by the keep-right bias. Improving the current condition is of much higher priority in congested conditions and hence the keep-right bias is generally neglected in such conditions. For simplicity, a constant value (say 0.1) can be chosen equal to I_{kr} in congested conditions which means the lane changes are restricted by this factor and the incentive is not completely neglected. The model is not affected in a major way if this incentive is completely neglected ($I_{kr} = 0$) in congested conditions. For lane changes towards the right, I_{kr} is chosen as zero in this case. Since vehicles generally return to their original lanes after overtaking, this assumption allows for vehicles to drive on the right-most lane and overtake when there is a gap thus obeying the keep-right rule implying that the vehicles eventually end up on the right most lanes due to this choice. The only exception to the above is for lane changes towards the right-most lane from the adjacent lane. Therefore, in this case (8) is used instead. Since the right-most lane is used also by heavy vehicles, drivers do not generally change lanes to the right-most lane as quickly as compared to other situations to avoid interactions with these heavy vehicles.

Route based incentive

The max operator in (6) ensures that any negative values are omitted. At lane drops, off-ramps, etc. where vehicles need to change lane to maintain their route (Mandatory Lane Changes (MLC)), simple
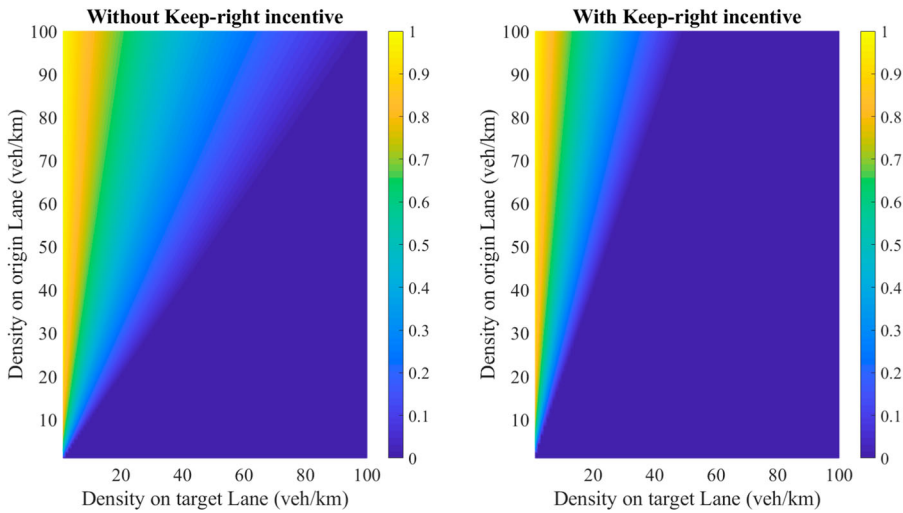
Figure 3. Lane change probabilities considering keep-right bias.

density or speed difference as a motivation is certainly not enough to compute lateral flows. In cases where vehicles need to change lane from a low density to a high density lane to maintain their route, the term IK_l in (6) should be greater than the density on the target lane for any lane change to occur. This is considered by the route incentive I_r. I_{kr} is equal to zero for the lanes on which route incentive term is active because the main priority of vehicles is to change lanes to maintain their route and not the keep-right action or a desire to change to a lower density lane. The term I_r should continue to increase as the distance to the end of the lane decreases because vehicles definitely need to change lane as they approach the end. Hence it is given by:

$$I_r = \left(1 - \frac{g}{D}\right)^3 \tag{10}$$

where, g is the distance to the end of the lane and D is the distance (a parameter) within which other incentives are neglected, i.e. maintaining route is the only criteria for lane change. This incentive is active only when g is less than or equal to D. It can be seen from (10) that the route incentive depends only upon the distance to the end of lane and not on the density difference after the distance g to the end of the lane is less than D. The cubic function in (10) was chosen as it represented a smooth and gradual increase in probability of lane changing initially followed by a rapid ascent when lane drop is almost approaching which mirrors the real world behaviour.

Cooperation incentive

In order to facilitate the merging of vehicles near the lane drop/on ramp sections, vehicles on the adjacent lane exhibit cooperative lane changing behaviour. Cooperative lane changing behaviour has been observed in many studies (Hidas 2005; Wang 2005). A similar approach used in the keep-right incentive is used to formulate the cooperation incentive. For the distance less than D, vehicles on the lane adjacent to a lane drop/ramp change lanes to create gaps for the merging vehicles. It is assumed that cooperative lane changing is possible only in free- flow conditions. The cooperation incentive is given as:

$$I_{coop} = \begin{cases} \frac{k_{l'} + k_l}{k_l} & g < D \\ 0, & g \geq D \end{cases} \tag{11}$$

Computation of longitudinal flows

Longitudinal flows are flows going from one cell segment to its immediate downstream cell segment in the same lane. From the CTM, the traffic flow transferred from the upstream cell i to downstream cell $i + 1$ in the case of a single lane section is given as:

$$q_{il}(t) = \min\{D_{il}(t), S_{i+1,l}(t)\} \tag{12}$$

The longitudinal flow is given as the minimum of demand D of cell i and supply S of cell $i + 1$. The total demand of a cell i in lane l is given by:

$$D_{il} = \min\{u_{il} * k_{il}, C_{il}\} \tag{13}$$

The time index is dropped from the equations that follow for clarity. In (13), u and C represent the free flow speed and capacity of the cell respectively. The flow that is expected to change lane from this cell will be a certain fraction of this demand. The lateral demand of cell i on lane l is then given as:

$$\varphi_{il \to l'} = D_{il} * Pr_{il \to l'} \tag{14}$$

The supply of cell $i + 1$ on lane l is equal to:

$$S_{i+1,l} = \min\{C_{i+1,l}, w_{i+1,l}(kjam_{i+1,l} - k_{i+1,l})\} \tag{15}$$

where, $kjam$ and w are the jam density and wave speed of the cell respectively. Since the cell on the adjacent lane can only accept a certain part of the lateral demand $\varphi_{il \to l'}$ based on its capacity, a parameter θ is calculated to restrict the lateral demand.

$$\theta_{il'} = \min\left[1, \frac{C_{il'} - S_{il'}}{C_{il'}}\right] \tag{16}$$

The actual lateral flow among cells is finally given as:

$$lq_{il \to l'} = \begin{cases} \varphi_{il \to l'}, \theta_{il'} = 1 \\ (1 - \theta_{il'}) * \varphi_{il \to l'}, \theta_{il'} < 1 \end{cases} \tag{17}$$

Capacity drop

While first order models are popular because of their computational efficiency and simplicity, an important phenomena commonly observed in real traffic but not reproduced by the early first order models is the Capacity Drop (CD). After the onset of congestion, the capacity reduces by a certain fraction and this difference in the queue discharge rate and actual capacity value is termed as capacity drop. Second and higher order models were developed to overcome this problem by including an additional dynamic equation which describes the speed evolution. Various extensions to first order model to incorporate capacity drop have since been proposed. The authors refer to Kontorinaki et al. (2017) for a more comprehensive discussion on this topic. In order to maintain the simplicity of the model, extensions with linear formulations were considered for use in our model. Han et al. (2016) provided an extension of first order model with a linear formulation in order to incorporate the capacity drop phenomena by modifying the supply function of the downstream cell in order to reflect the reduced flow discharge during congestion. This was an extension of a similar method employed by Roncoli, Papageorgiou, and Papamichail (2015) where the demand function is linearly modified instead of the supply function. The approach used by Han et al. (2016) is used to incorporate CD in the model. The formulation is described in brief here. For more details, the authors refer to the original paper. In this extension, when the density of cell i is greater than the critical density of cell $i + 1$,
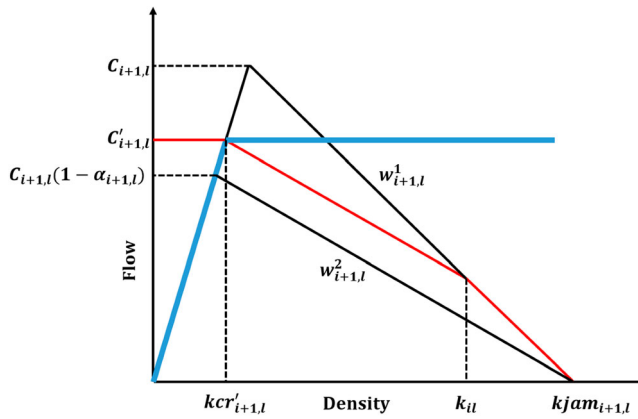
Figure 4. Demand (thick blue) and supply (red) of the proposed extension.

it is assumed that the capacity drops and the demand and supply functions are modified accordingly which are represented in Figure 4.

The equations for the demand and supply of the cell are modified as follows:

$$S_{i+1,l} = \min\{S_{i+1,l}^1, S_{i+1,l}^2, C'_{i+1,l}\} \tag{18}$$

$$S_{i+1,l}^1 = w_{i+1,l}(kjam_{i+1,l} - k_{il}), k_{il} \leq k_{i+1,l} \tag{18a}$$

$$S_{i+1,l}^2 = w_{i+1,l}(kjam_{il} - k_{il}) + \frac{C_{i+1,l}(1 - \alpha_{i+1,l})}{kjam_{i+1,l} - kcr'_{i+1,l}} * (k_{il} - k_{i+1,l}) \tag{18b}$$

$$C'_{i+1,l} = C_{i+1,l}\left(1 - \alpha_{i+1,l} * \left(\frac{k_{il} - kcr_{il}}{kjam_{il} - kcr_{il}}\right)\right) \tag{18c}$$

$$D_{il} = \min\{k_{il} * u_{il}, C'_{il}\} \tag{19}$$

where, $\alpha_{i+1,l}$ is the extent of the capacity drop and kcr is the critical density of the cell segment. Hence, these modified supply and demand functions (18 and (19)) will be used when the cell is in a discharging state ($k_{il} \geq k_{i+1,l}$). In all other cases, (13) and (15) will be used.

Since, lateral flows are computed before the longitudinal flows, there effect on the overall longitudinal flow have to be taken into account. However, it must be remembered that the order of computation does not affect the results as long as the both the flows are computed and allotted within the same time step and the initial order is maintained throughout all the time steps.

$$mod\_D_{il} = D_{il} + lq_{i,l'\rightarrow l} - lq_{i,l\rightarrow l'} \tag{20}$$

$$mod\_S_{i+1,l} = S_{i+1,l} + lq_{i+1,l'\rightarrow l} - lq_{i+1,l\rightarrow l'} \tag{21}$$

The overall flow being transferred from one cell to the next in the longitudinal direction is then given as

$$Aq_{il}(t) = \min\{mod\_D_{il}, mod\_S_{i+1,l}\} \tag{22}$$

There is much debate on the magnitude of the capacity drop (Chung, Rudjanakanoknad, and Cassidy 2007; Yuan et al. 2017). For the sake of simplicity, in this paper, we will assume a capacity drop of 10% which leads to the value of α_{il} being 0.1.
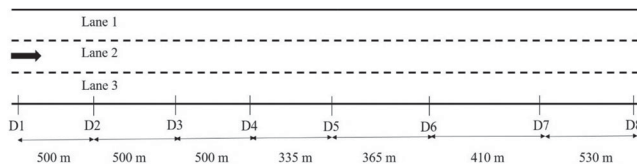
Figure 5. Representation of the A13 homogenous stretch.

Case study

The traffic flow model presented in the previous section is tested on two different motorway locations – a homogenous stretch on A13 motorway of The Netherlands and a lane drop section on A12 also located in The Netherlands. Homogenous sections are used to evaluate the performance of the model in its ability to reproduce the lane flow distributions. Since there are no discontinuities within homogenous sections, the lane changes within this section can be classified as Discretionary Lane Changes (DLC) where the primary motivation to change lanes is to improve the current condition. Lane-drop sections are used to evaluate the performance of the model when simple incentives applicable in DLC are no more valid. Since the vehicles have to change lane and merge to continue on their route, these lane changes can be classified as Mandatory Lane Changes (MLC). The two sections represent the two general types of lane changes which are DLC and MLC and hence chosen for study.

In this section, the details of the chosen study sites and data used, approach used for the estimation of FD parameters from this data and description of the statistical regression model which will be used as a benchmark to compare the developed model will be discussed. Results will follow in the next section.

A13 homogenous section

The purpose of choosing a homogenous section is to verify if the developed model can model lane flow distributions accurately when there are no discontinuities in the road stretch and the only incentive to change lane is to improve the current condition. Since the only motivation to change lane is to improve the current condition, route and courtesy incentives are excluded from (7). For the homogenous road stretch, we select the A13 motorway from The Hague to Rotterdam. The considered section, in Figure 5 is 3 km long and consists of three lanes. The section starts downstream of an on-ramp at 13.2 KP and ends upstream of an off-ramp around 16.2 KP in the direction of Rotterdam. This section is free from any infrastructural bottlenecks such as lane drops, ramp sections, etc. There are a total of 8 detectors on this 3 km long section. A time step of $\Delta t = 1s$ is used for simulation and following the CFL condition given in (4), the length of the cell segments is taken as 30 m which results in a total of 100 cell segments. Figure 5 shows the configuration of the network and detector locations. The lanes are numbered 1–3 starting from the median lane to the outer lane. The same convention in the numbering of lanes (i.e. lane numbers ascending from median/left-most lane) is followed in the rest of the paper. Traffic data from the upstream and downstream most detectors is used to supply the model with boundary conditions. Flow information from detector D1 is used to provide the demand entering the section and densities from detector D8 censor the flows exiting the section. Data for the month of March 2018 from 06:00 to 10:00 is used for testing the model. For the data available, it was observed that congestion never originated inside the considered stretch and usually propagated from a bottleneck downstream of the considered stretch. Since these effects are difficult to consider in the model as the exact cause of congestion outside the stretch is unclear, these days are neglected from analysis. Whenever the speeds at the downstream detectors of the stretch were below 60 km/h, it was assumed that congestion propagated outside the section and these days were excluded. Hence, the model was only tested in free-flow conditions for 10 days of this month on this homogenous stretch.
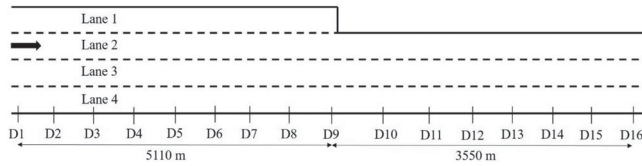
Figure 6. Representation of the A12 lane drop stretch.

A12 lane drop section

The model is also tested at a lane drop location where the motivation to change lanes at the vicinity of the lane drop is not just dependent upon the density difference across lanes. For this purpose, a lane drop bottleneck on the A12 motorway is selected. The lane drop near Woerden (40.65 KP) is used for testing the model. The total length of the segment was around 8.7 km with a left lane drop from 4 to 3 lanes after about 5.1 km. A total of 16 detectors were present on this section. This stretch was chosen because of its relatively long distance and absence of any interacting bottlenecks. Figure 6 shows a graphical representation of the section. Similar to the A13 case, the information from detectors D1 and D16 are used to supply the model with boundary conditions in the form of entering demands on each lane and densities at the exit locations. Data for the month of May 2007 from 15:00 to 19:00 h is used for calibrating and validating the model and similar to A13, days where congestion originated outside the considered stretch were excluded from analysis. Hence, 15 days from this month were used for analysis.

Fundamental diagram (FD) calibration

The 3 FD parameters (*u,w* and *kjam*) for the considered locations were calibrated using an optimization based approach where a cost function is minimized. The critical density of cells is a derived parameter and is equal to the density at the capacity of the cell. The capacity of cells is given by (23).

$$C = \frac{u.w.kjam}{u + w} \tag{23}$$

The FD parameter set δ^* containing the lane-specific free-flow speeds, wave speeds and jam density is obtained by:

$$\delta^* = \underset{\delta}{\mathrm{argmin}} \left[\sqrt{\sum_i^n \sum_j^L (k_{est,l}^i - k_{obs,l}^i)^2} \right] \tag{24}$$

where, *L* is the number of lanes and *n* is the number of observations. The cost function represents the difference between the estimated values of densities from the model and actual values measured at the various detectors. Hence, the parameters were bounded between certain reasonable ranges and a constrained optimization approach was followed. The optimization problem is solved by MATLAB implementation of the interior-point algorithm (`fmincon`). For example, the values of wave speed were restricted to [15, 25] km/h range since higher or lower values are rarely observed or unrealistic. Similarly, the bounds for free-flow speed and jam density were obtained from the q-k scatter plots of the detector data. Such a constrained approach yielded parameter values which were much more realistic as opposed to the unconstrained approach. Data from an arbitrarily chosen day (16 March 2018 in this case) is used for estimating the FD parameters for the A13 stretch. The remaining days are used for validating the model. 1-minute aggregated speed and flow information from stationary lane based detectors were used to compute densities. The traffic flow models generally use speeds that are space-mean but the measure speeds are time-mean. Stationary detector data (SDD) do not allow for an unbiased estimate of the density (Treiber and Kesting 2013). While this should not affect

Table 1. A13 FD parameters.

	Free-flow speed u (km/h)	Wave speed w (km/h)	Jam density k_{jam} (veh/km)
Lane 1	104.6	19.5	162
Lane 2	98.5	21.4	140
Lane 3	87	20	120

Table 2. A12 FD parameters.

	Free-flow speed u (km/h)	Wave speed w (km/h)	Jam density k_{jam} (veh/km)
Lane 1	117.6	22.6	133
Lane 2	116.6	22.5	149
Lane 3	110	22	132
Lane 4	94.8	17.6	103
Lane 2 (after LD)	103	20	169
Lane 3 (after LD)	99.3	20	155
Lane 4 (after LD)	92.5	20.6	97

the results in free-flow conditions, there is a possibility to underestimate density by a factor of almost 2 in congested conditions (Knoop, Hoogendoorn, and van Zuylen 2009). Since the main scope of the paper is to evaluate the incentive based formulation, for simplicity, time-mean speeds are used in the model. The parameters of the lane-specific FDs for this road section are given in Table 1.

In the case of the lane drop section on A12, parameters from 7 lane specific FDs were required to be estimated. The 7 FDs include the 4 FDs upstream and 3 FDs downstream of the lane drop on each lane. This implies that 21 parameters need to be estimated using the optimization approach which can be computationally intensive but unavoidable especially considering lane specificity. Detector data of 6 May 2007 is used for the calibration of FD parameters. The distance parameter D described in (10) is taken as 750 m. Initial sensitivity analysis showed that higher values of D such as 1000 m lead to worse performance of the model and lower values are generally not preferred as drivers like to be in the right lanes at least 500 m upstream of the end of the lane (Keyvan-Ekbatani, Knoop, and Daamen 2016). Hence a value of 750 m was chosen avoiding the need for the calibration of an extra parameter. The parameters for this stretch are given in Table 2.

Performance indicator

Using the FD parameters resulting from the calibration process, the model is tested for different days in order to demonstrate the validity of the model. Weighted density was used while considering density difference across lanes for calculating the lane change rates where information of the two downstream cells (apart from the current cell) was used in order to consider the effect of downstream conditions. Initial sensitivity analysis showed that the error values were indeed lower when downstream conditions were taken into account. The root-mean-square-error (RMSE) values of the densities at the various detectors are used as a metric to measure the performance of the model and compare it to the linear regression models. The RMSE is given by the equation:

$$\text{RMSE} = \left[\sqrt{\sum_i^n \sum_j^L (k_{est,l}^i - k_{obs,l}^i)^{\wedge}2} \right] \tag{25}$$

Linear regression (LR) model

A naïve statistical model is used as a benchmark to compare the performance of the developed traffic flow model. Naïve approaches are generally cost-effective and provide a benchmark against which more sophisticated models can be compared. Linear Regression models are used for this purpose as it

is one of the simplest methods used for forecasting considering the time-series data available from the detectors (Neter et al. 1996). For the LR model, the density of a detector is assumed to be dependent upon the densities of its upstream and downstream detectors as well as its corresponding detector on the neighbouring lane. In order to maintain consistency for comparison, both the traffic flow model and the regression model are provided with the same information. The linear regression equation for a certain detector from Figure 5 (for, e.g. detector 2 on lane l) is given by:

$$k_{D2,l} = \beta_0 + \beta_1 * k_{D1,l} + \beta_2 * k_{D3,l} + \beta_3 * k_{D2,l'}$$ (26)

where $\beta_0, \beta_1 \ldots ..\beta_n$ are the coefficients, $k_{Di,l}$ is the density in the origin lane and $k_{Di,l'}$ is the density in the neighbouring lane. In order to estimate the coefficients, detector data from the previous days is used and these estimated coefficients are used to predict the densities for the chosen day. For example, if the densities are to be predicted for March 16, data from the previous 15 days is used for estimating the coefficients using the linear regression approach and then (26) is used to predict the densities for March 16. A 5 min moving average of the densities for the past data is used while estimating the coefficients to filter out the random fluctuations. Another variation of this model is also used for comparison where the information from the detector on the adjacent lane is not used. In this case, the following equation is used for detector 2.

$$k_{D2,l} = \beta_0 + \beta_1 * k_{D1,l} + \beta_2 * k_{D3,l}$$ (27)

The final term in (26) containing information about the densities on the adjacent lane is omitted in (27) to see if it plays any role in enhancing the performance of the regression model.

Results

The model is applied to the two road stretches described in the previous section and the results are discussed here.

Lane-flow distribution and density plots for A13

The model is validated against data from different days using the parameters resulting from the calibration process. It was observed that the model was able to replicate the lane change dynamics on this stretch for all the days. For visualization purposes, we present the results of a one day (21 March 2018). The lane flow distribution across the lanes for the A13 stretch on this day is shown in Figure 7. The lines with marker show the median of the fractions in the chosen bin sizes and the unmarked lines surrounding them represent the error margins within one standard deviation. Data from all 6 detectors (i.e. from D2 to D7) were used to plot the lane flow distribution. The model is able to replicate the lane flow distribution patterns generally observed on 3-lane motorways (Wu 2006; Knoop et al. 2010). The decrease and increase in the fraction of flow with increasing roadway density on lanes 3 and I respectively are well represented by the model. The lane flow distribution on the three lanes also converge at around the same roadway density in both the actual data as well as in the estimated results. The model results shows good resemblance to the actual data though there are a few differences. One which can be clearly observed is the magnitude of rise or drop in the fraction of flow on all the lanes with increasing roadway density. Another point of difference is the flow distribution of the centre lane. According to the model, the flow increases (very slightly) on the centre lane with increase in roadway density which is not the case in the actual data. Some of the reasons which contribute to the difference in magnitude include (a) absence of stochasticity in the model which can lead to less scatter and hence the difference in the magnitude of rise or drop in the fraction of flow (b) sensitivity of the model results to the FD parameters and shape of the FD restricting the values within certain bounds (c) boundary conditions at the upstream and downstream end of the section. As has been previously mentioned, there is an on-ramp upstream of the start of the section and an off-ramp
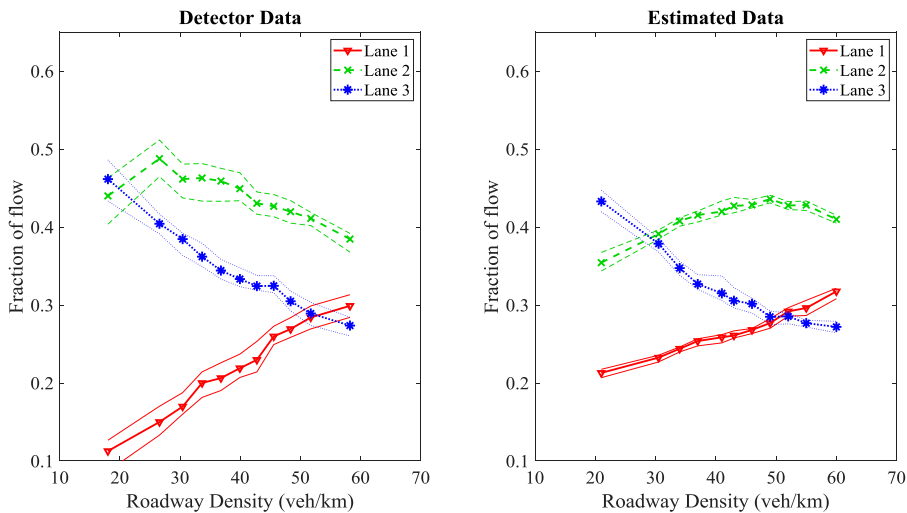
Figure 7. Comparison between observations and estimations of lane flow distribution (A13).

immediately downstream. This cannot be considered in the model as it is outside the section. This can also impact the lane flow distribution due to the lane change activity near these boundaries. Other possibilities might also include the formulation of the keep-right incentive which affects the lane flow distribution. At low-flow conditions, the criterion for the keep-right incentive is causing the flow to move from lane 1 to lane 2 while restricting the flow to remain on lane 2 and not move to lane 3 which causes the relatively high fraction of flow. Also, the role of heavy vehicles (generally found on lane 3) is not considered in the model which might affect the lane flow distribution. The promising aspect to be observed in this that the model can definitely reproduce the distribution patterns generally observed on 3-lane motorways.

Figure 8 shows the comparison of the time-series of densities on the three lanes of A13 between the actual data and the estimated results for 21 March 2018. It can be seen that the model results closely resemble the detector data observed. This trend is maintained for all the detectors though there are some variations between the model results and real world data for D7 which is to be expected considering that there is an off-ramp downstream of the boundary of the considered stretch. Hence, near the end of the section, lane changing motivation is not just dependent upon improving the situation but also on maintaining the route.

Density time-series plots for A12

The density time series plots of two detectors upstream and downstream of the lane drop on the A12 stretch for 12 May 2007 are shown in Figure 9. No congestion was observed in the stretch on this day. It can be observed that the model results closely resemble the actual detector information. On lane 1 upstream of the lane drop, the model predicts comparatively higher densities than observed. This implies that according to the model, higher number of lane changes take place quite near the lane drop than is actually observed. The model also predicts higher values of densities on Lane 2 downstream of the lane drop. Generally, higher densities are to be expected on Lane 2 downstream of the lane drop due to merging of vehicles near the bottleneck. But in the actual case, densities are quite low on Lane 2 downstream of the lane drop. A reason that can be attributed to this is due to the cooperative lane changing behaviour of drivers before the lane change. Although a cooperation incentive is included in the lane change function, the criteria for the execution of this incentive is quite rigid which can be a reason for the lower number of cooperative lane changes in the model results. Being free-flow conditions, vehicles may have executed cooperative lane changes to allow vehicles to merge near the
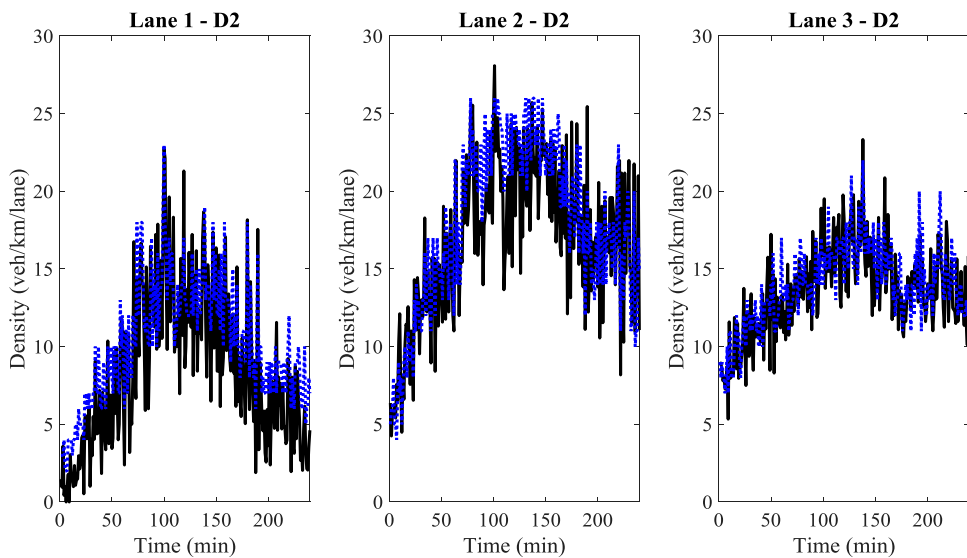
Figure 8. Comparison between detector data (blue dotted line) and model results (black) – A13.

lane drop and avoid any congestion in the actual data. The results also show that lane usage at D9 and further slowly drops to zero on Lane 1 which shows that the route incentive works well.

The model was also validated against congested conditions for the lane drop stretch. The model results are compared to the data from 22 May 2007. On this day, congestion was observed to originate from the lane drop and extend several kilometres upstream. The cause of congestion is the excess demand. From Figure 10, it can be seen that the demand exceeds the bottleneck capacity after $\sim$ 50 mins and remains high for a period of 2.5 hrs. The capacity of the bottleneck is calculated from the calibrated set of FD parameters. This leads to the onset and growth of congestion on this stretch. Since there are no other bottlenecks in the vicinity, the congestion observed in this stretch can be attributed to the lane drop. Congestion starts at approximately 4 pm and continues almost till 6:30 pm. In The Netherlands, when the speeds detected on a motorway fall below a threshold value, Variable Message Signs (VMS) are activated recommending lower speeds in order to avoid rear-end collisions of drivers crashing into the tail of the traffic jam. Upon the activation of VMS, drivers tend to slowly reduce their current speed anticipating congestion downstream of their location. This affects the shape of the FD locally and temporally (Zhang 1999) since the free-flow speed and other parameters are varied which the model does not take into consideration.

Since the model does not take into account the driver reaction to VMS and their anticipatory behaviour in such scenarios while estimating the densities, the results will be different to those actually observed. For a detailed discussion on the effect of human factors on the fundamental diagram, the authors refer to Ni et al. (2017). The comparison between the estimated results and the actual detector data for a particular detector (D8) is shown in Figure 11. It can be observed that in the actual case, densities keep fluctuating after the onset of congestion. As the model does not take into account changing FD parameters, there are no fluctuations observed in the model results. But the model can indeed estimate the time at which the congestion begins on the lanes which can be seen from the rise in densities at almost the same time compared to the real world data. The density drops on all the lanes at around the 3 hr mark in the model results which is line with the drop in demand compared to the bottleneck capacity at this time. Hence, the model does work even in congested conditions. The duration of congestion predicted by the model, however, differs from the observations by around an hour. The model is able to produce the onset and propagation of congestion till the end of the 3rd hour (180th minute). The mismatch in the duration of congestion can be explained by the 'memory
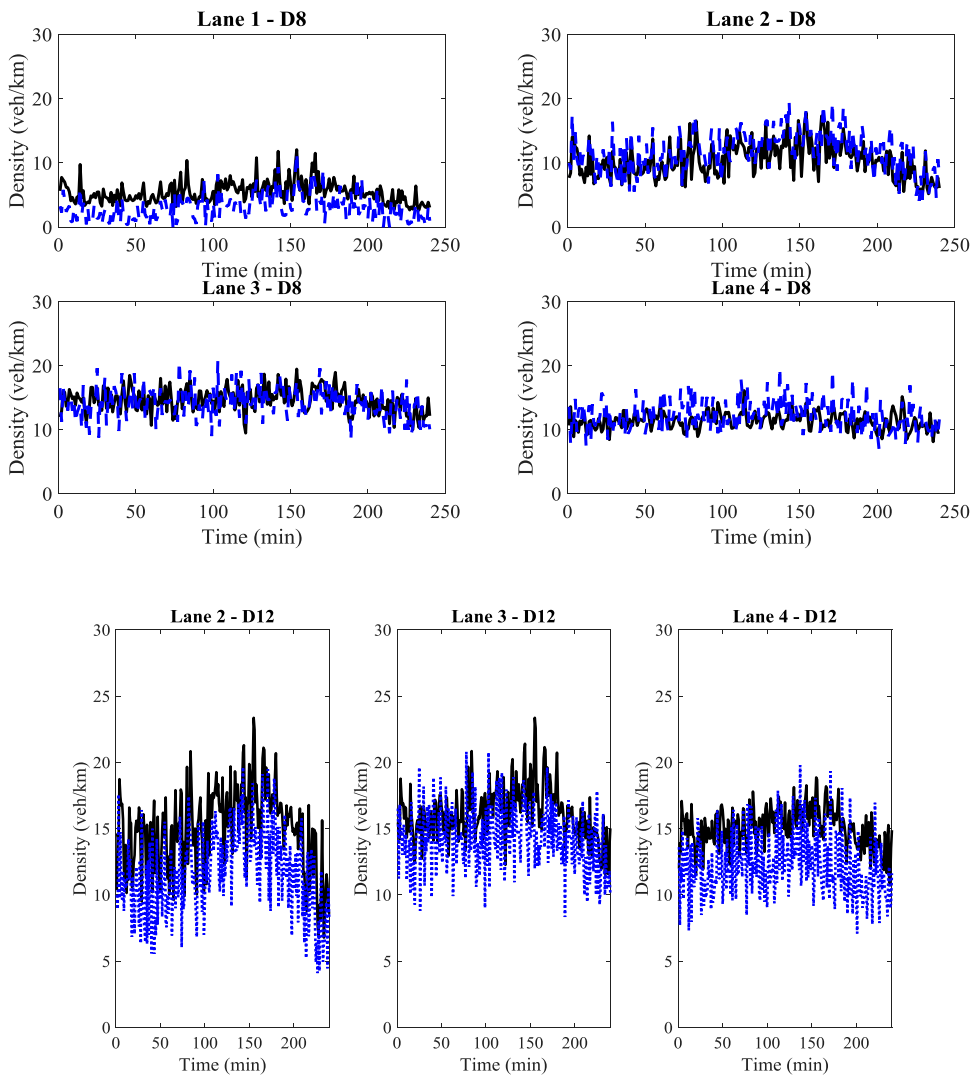
Figure 9. Comparison between detector data (blue dotted line) and model results (black solid) for May 12th, 2007 – A12.

or resignation effect' which was quantified using a microscopic car-following model in Treiber and Helbing (2003).

Drivers tend to get less responsive as they remain in a jam for a long time causing the driver to adapt and increase the net time gap in response to the surrounding traffic environment. This leads to a reduction in capacity. This effect can be introduced macroscopically by introducing a dynamic variable to reduce the absolute value of the wave speed *w* as a function of the jam length or duration of congestion similar to the adaptation of net time gap in the original work to account for the varying capacity in congestion.

The higher magnitude of the densities estimated by the model in relation to observed values on lane 4 can be attributed to the formulation of the keep-right incentive in congested conditions which can lead to higher flows on lane 4.

The lane change (LC) rates are also evaluated for this day. Figure 12 shows the LC rates upstream of the lane drop bottleneck. Due to the absence of information regarding the number of lane changes in the real-world data, a direct comparison of estimated lane change rates with actual lane change rates
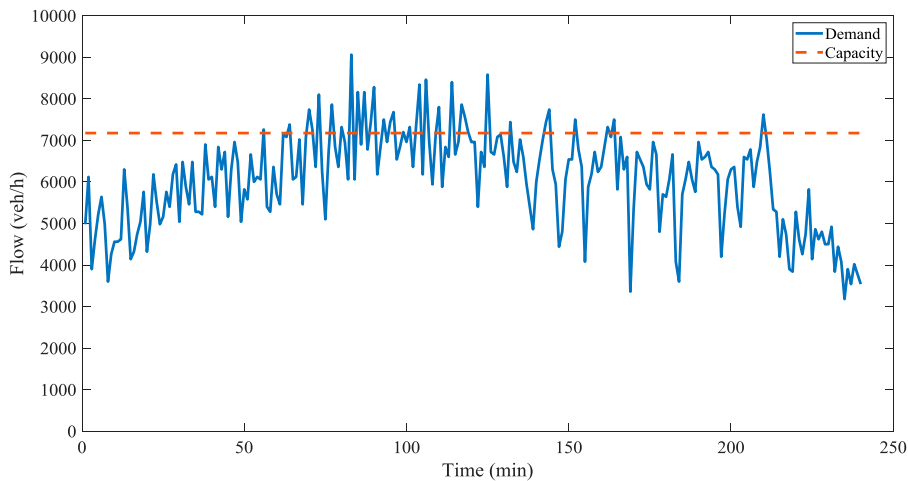
Figure 10. Demand vs Bottleneck capacity for May 22nd, 2007.
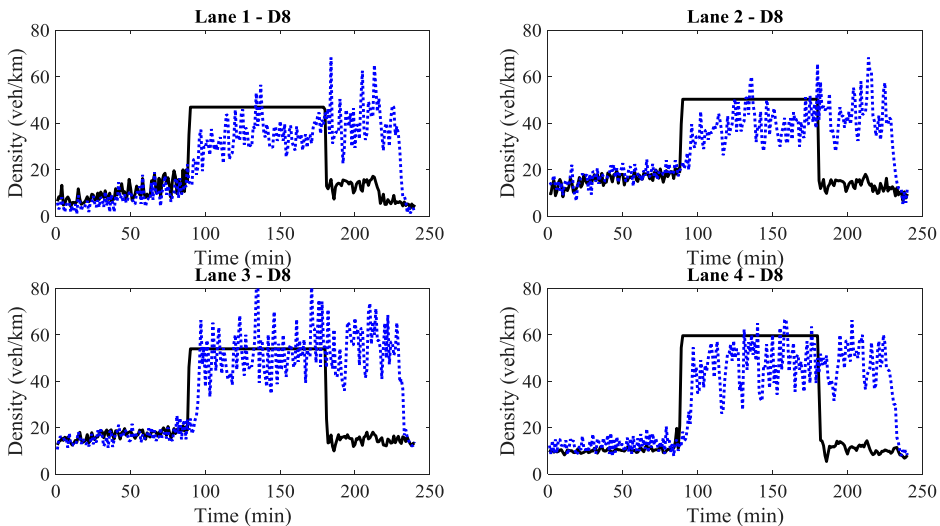

Figure 11. Comparison between detector data (blue dotted line) and model results (black solid) for May 22nd, 2007 – A12.

observed is not possible. However, the values of the LC rates obtained are quite consistent with those observed in the empirical studies by Knoop et al. (2012) and Guo, Wu, and Zhu (2018). Knoop et al. (2012) observed a LC rate of 0.2–0.5 $veh^{-1}km^{-1}$ on a motorway in the Netherlands. But the considered stretch was a homogenous one and the effect of mandatory lane changes (MLC) on the LC rate is not studied. Guo, Wu, and Zhu (2018) observed higher values in their study ranging from 0.3–1.5 $veh^{-1}km^{-1}$. In this study, the considered stretch took into effect the presence of on/off ramps and they attribute the high LC rates to the aggressive lane changing at these locations.

It can be seen from Figure 12 that as the lane drop approaches, the LC rates continuously increase with a high value of $\sim$ 1.5 $veh^{-1}km^{-1}$ immediately upstream of the bottleneck. This can be attributed to the high lane changing activity arising from the need to change lanes from lane 1–2 and the subsequent induced lane changes on the other lanes. Similar patterns are observed for other days. The estimated LC rates align well with the values observed in the aforementioned studies.
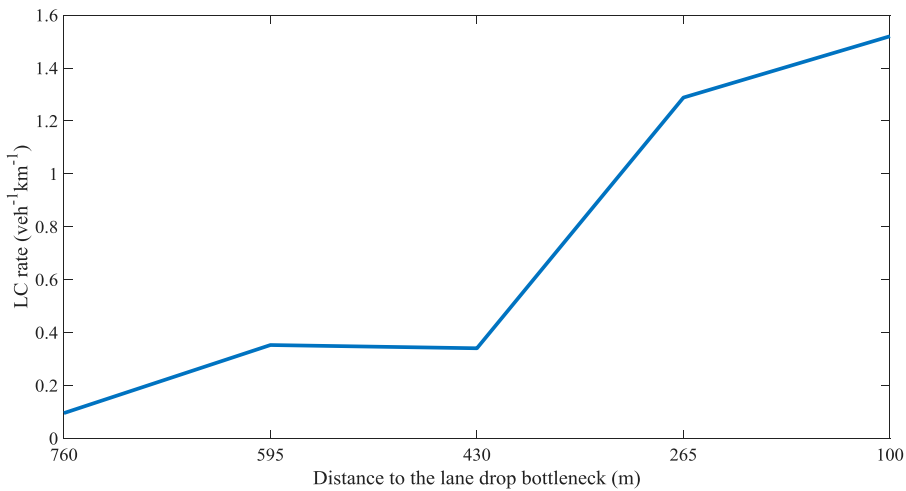
Figure 12. LC Rates upstream of the lane drop – May 22, 2007.

Comparison with the LR models

Using RMSE as a metric, the model results are compared to the LR models described in section 4. Figure 13 shows the comparison between the RMSE values of the densities on various lanes obtained from the traffic flow model and the LR models on the A13 stretch for 21 March 2018. Error values range between 2–3 veh/km/lane for the proposed traffic flow model. Comparing the model to the LR models for this stretch, it can be seen that the traffic flow model outperforms the regression models on all the lanes. It can also be seen that using the detector information from the adjacent lanes in the regression model does not seem to reduce the error by much and the two regression models almost lead to similar results. Due to the presence of an off-ramp at the end of the stretch, more lane changing activity is expected to take place towards Lane 3 which is not accounted for in the model for this stretch. This lead to increasing error values at detectors D6 and D7 on Lane 3 in all the models.

The comparison between the traffic flow model and the LR models for 12 May 2007 on A12 lane drop is given in Figure 14. The vertical line in these plots represents the location of lane drop which is between detectors D9 and D10. It can be observed that the traffic flow model performs better than the benchmark models in general. On Lane 1, the regression model without neighbouring detector information seems to result in the least error values. The model does not seem to work particularly well on the Lane 2 downstream of the lane drop which can be seen from the rising error values. One of the reasons already mentioned is the lack of a well-defined cooperative lane changing component in the incentive function. Another reason could be the sensitivity of the results to the FD parameters. By changing the FD parameters on Lane 1, errors on this lane could be reduced. But this affects the results negatively on the other lanes. The calibrated FD parameters used for validation give rise to the least overall error based on the defined cost function in (24) rather than lane-specific minimum errors. On average, the traffic flow model performs much better than the LR models.

Figure 15 shows the heat map of the RMSE of densities for 22 May 2007 when congested conditions were observed due to the lane drop bottleneck. It can be seen that the error values are very high upstream of the lane drop. Especially on lanes 3 and 4, error values are in the range of $\sim$20 veh/km which is extremely high. The reason for this has already been highlighted in the previous sub-section. The extremely high value of $\sim$40 on lanes 3 and 4 at D9 is due to the absence of detector data on these lanes for this day. For this particular day and location, the LR models perform better than the traffic flow model but they also result in high error values in the range of 10–15 veh/km. However, the important point to remember is that the model can indeed represent the onset and propagation of congestion.
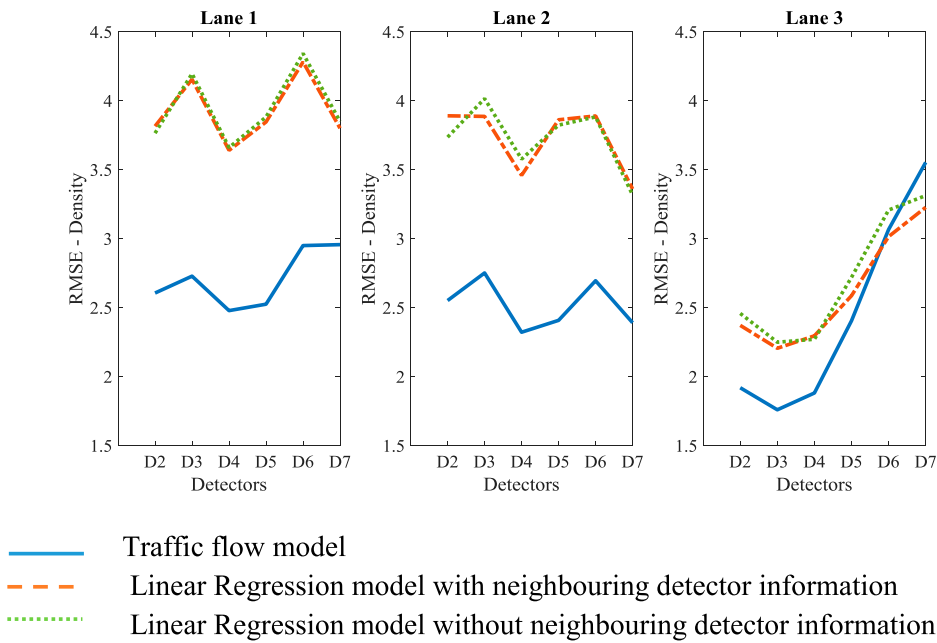
Figure 13. Comparison of RMSE (densities) between traffic flow model and LR models – A13.
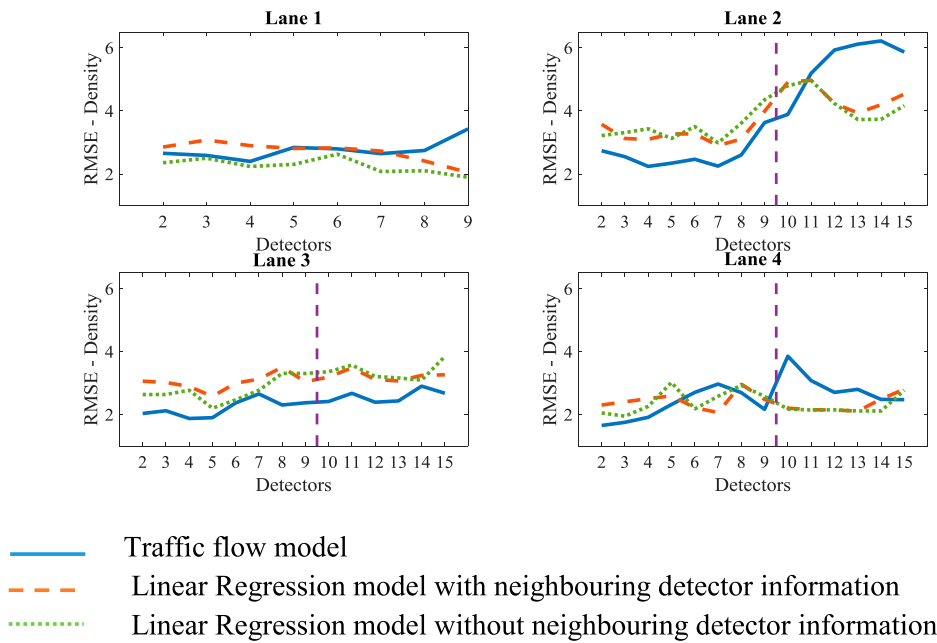

Figure 14. Comparison of RMSE (densities) between traffic flow model and LR models – A12.

Discussions

In this section, we discuss the sensitivity of the results of the traffic flow model to the values of the FD parameters. The model consists of a number of parameters such as lane-specific free-flow speeds, jam densities and wave speeds. The accuracy and reliability of the model depends upon the set of
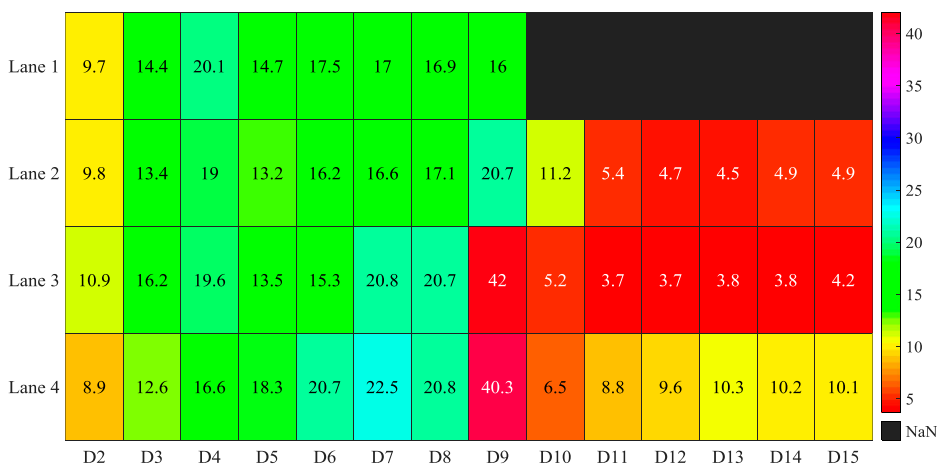
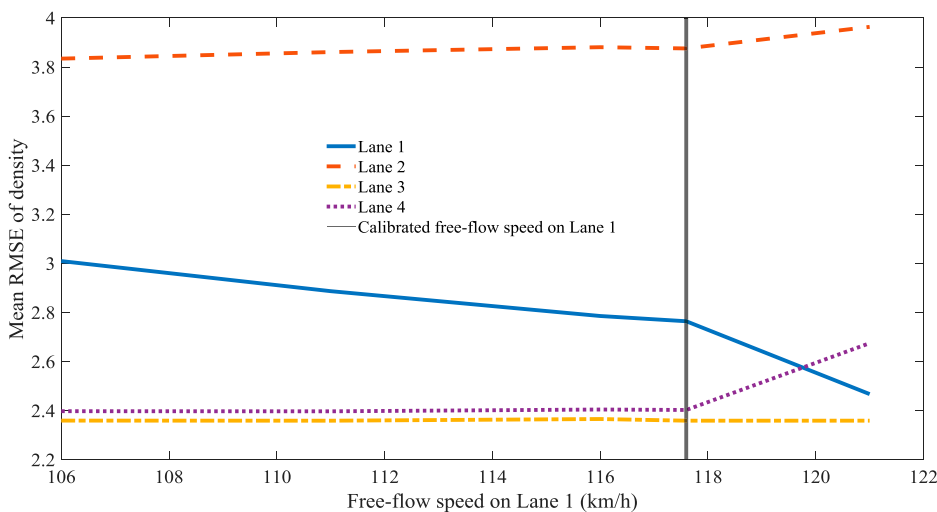**Figure 15.** Heat Map of the RMSE of density for May 22nd, 2007.

Figure 16. Variation of RMSE with respect to free-flow speed on Lane 1.

parameter values used. In the A12 lane drop stretch, it was observed in Figure 14 that the error values on Lane 2 increases just upstream and downstream of the bottleneck. In a lane drop section, this lane is of much importance due to the high lane changing activity to and from this lane. While the function for computing the lane change rates can be a source of this increasing error value, another possibility is the dependence of the results on the values of FD parameters. In this study, the FD parameters were calibrated using an optimization based approach where the objective was to minimize the sum of errors across the lanes. Although this leads to a set of parameter values which leads to the least sum of errors across all the lanes, it might not always lead to the best results for a particular lane.

Figure 16 shows the variation of mean RMSE of density on each lane with respect to different values of the free flow speed on Lane 1. It can be observed from the figure that by varying the free-flow speed on Lane 1, the results on other lanes can be varied. The performance of the model on lane 1 improves with increasing free flow speed on its lane but deteriorates on lane 2 and lane 4. There is not much variation in the results of lane 3. Change in free-flow speed of Lane 1 not only affects its adjacent lane but the innermost lane (lane 4) too. Though not represented in the figure, the overall mean RMSE

across lanes decreases (albeit very slightly) till the optimum free-flow speed of lane 1 represented by the dotted vertical line and increases again. Hence, the model results are sensitive to the chosen set of parameters. One way of resolving this is by assigning weights to the individual errors of each lane in the objective function with more weightage to lanes of higher importance in terms of traffic control (such as lanes 1 and 2 for the A12 stretch).

Conclusions

A first order multi-lane traffic flow model was developed considering various incentives such as density difference, maintaining route, keep-right bias for lane changing motivation. The function to compute lane change rates across cell segments in different lanes with these incentives was introduced without the addition of any additional parameters. The model was tested against real world data collected from two different sites. The fundamental diagram parameters were calibrated from the detector data of these two sites. It has been shown that the model can notably estimate the lane flow distribution across the lanes. Even though there a limited number of parameters, the developed model outperforms the linear regression models. The model also worked well in congested conditions. The developed model worked well for a variety of lane change scenarios due to the incentive formulation and can be used in a control framework to find ideal lane change rates and locations to mitigate congestion and achieve a balanced lane usage.

While the results of the model are indeed promising, there are some limitations. The model results are sensitive to the FD parameters and cannot take into account changing FDs resulting from driver anticipatory behaviour. A feedback system such as the Kalman filter (and its extensions) used by Wang and Papageorgiou (2005) or an automatic fitting procedure as described in Knoop and Daamen (2017) can be used for the estimation of FD parameters. The model is also restricted to isolated bottlenecks. In the future, the model will be extended to consider interacting bottlenecks where the lane changing motivation is a function of multiple interacting incentives and not just dependent upon a single incentive.

Disclosure statement

No potential conflict of interest was reported by the authors.

Funding

References

Chung, K., J. Rudjanakanoknad, and M. J. Cassidy. 2007. "Relation Between Traffic Density and Capacity Drop at Three Freeway Bottlenecks." *Transportation Research Part B: Methodological* 41 (1): 82–95.

Daganzo, C. F. 1994. "The Cell Transmission Model: A Dynamic Representation of Highway Traffic Consistent with the Hydrodynamic Theory." *Transportation Research Part B: Methodological* 28 (4): 269–287.

Duret, A., S. Ahn, and C. Buisson. 2012. "Lane Flow Distribution on a Three-Lane Freeway: General Features and the Effects of Traffic Controls." *Transportation Research Part C: Emerging Technologies* 24: 157–167.

Gipps, P. G. 1986. "A Model for the Structure of Lane-Changing Decisions." *Transportation Research Part B: Methodological* 20 (5): 403–414.

Guo, M., Z. Wu, and H. Zhu. 2018. "Empirical Study of Lane-Changing Behavior on Three Chinese Freeways." *PloS One* 13 (1): e0191466.

Han, Y., Y. Yuan, A. Hegyi, and S. P. Hoogendoorn. 2016. "New Extended Discrete First-Order Model to Reproduce Propagation of jam Waves." *Transportation Research Record* 2560 (1): 108–118.

Hidas, P. 2005. "Modelling Vehicle Interactions in Microscopic Simulation of Merging and Weaving." *Transportation Research Part C: Emerging Technologies* 13 (1): 37–62.

Jin, W. L. 2010. "A Kinematic Wave Theory of Lane-Changing Traffic Flow." *Transportation Research Part B: Methodological* 44 (8-9): 1001–1021.

Jin, W. L., and J. Laval. 2018. "Bounded Acceleration Traffic Flow Models: A Unified Approach." *Transportation Research Part B: Methodological* 111: 1–18.

Kesting, A., M. Treiber, and D. Helbing. 2007. "General Lane-Changing Model MOBIL for car-Following Models." *Transportation Research Record* 1999 (1): 86–94.

Keyvan-Ekbatani, M., V. L. Knoop, and W. Daamen. 2016. "Categorization of the Lane Change Decision Process on Freeways." *Transportation Research Part C: Emerging Technologies* 69: 515–526.

Knoop, V. L., and W. Daamen. 2017. "Automatic Fitting Procedure for the Fundamental Diagram." *Transportmetrica B: Transport Dynamics* 5 (2): 129–144.

Knoop, V. L., A. Duret, C. Buisson, and B. Van Arem. 2010. "Lane Distribution of Traffic Near Merging Zones Influence of Variable Speed Limits." Paper presented at the 13th International IEEE Conference on Intelligent Transportation Systems.

Knoop, V. L., S. P. Hoogendoorn, Y. Shiomi, and C. Buisson. 2012. "Quantifying the Number of Lane Changes in Traffic: Empirical Analysis." *Transportation Research Record: Journal of the Transportation Research Board* 2278: 31–41.

Knoop, V., S. P. Hoogendoorn, and H. van Zuylen. 2009. "Empirical Differences Between Time Mean Speed and Space Mean Speed." In *Traffic and Granular Flow'07*, edited by C. Appert-Rolland, F. Chevoir, P. Gondret, S. Lassarre, J. P. Lebacque, and M. Schreckenberg, 351–356. Berlin, Heidelberg: Springer.

Kontorinaki, M., A. Spiliopoulou, C. Roncoli, and M. Papageorgiou. 2017. "First-order Traffic Flow Models Incorporating Capacity Drop: Overview and Real-Data Validation." *Transportation Research Part B: Methodological* 106: 52–75.

Laval, J. A., and C. F. Daganzo. 2006. "Lane-changing in Traffic Streams." *Transportation Research Part B: Methodological* 40 (3): 251–264.

Michalopoulos, P. G., D. E. Beskos, and Y. Yamauchi. 1984. "Multilane Traffic Flow Dynamics: Some Macroscopic Considerations." *Transportation Research Part B: Methodological* 18 (4-5): 377–395.

Munjal, P. K., and L. A. Pipes. 1971. "Propagation of on-Ramp Density Waves on Uniform Unidirectional Multilane Freeways." *Transportation Science* 5 (4): 390–402.

Neter, J., M. H. Kutner, C. J. Nachtsheim, and W. Wasserman. 1996. *Applied Linear Statistical Models, Vol. 4*. Chicago: Irwin.

Ni, D., L. Li, H. Wang, and C. Jia. 2017. "Observations on the Fundamental Diagram and Their Interpretation From the Human Factors Perspective." *Transportmetrica B: Transport Dynamics* 5 (2): 159–176.

Pan, T. L., W. H. Lam, A. Sumalee, and R. X. Zhong. 2016. "Modeling the Impacts of Mandatory and Discretionary Lane-Changing Maneuvers." *Transportation Research Part C: Emerging Technologies* 68: 403–424.

Pan, T., W. H. Lam, A. Sumalee, and R. X. Zhong. 2019. "Multiclass Multilane Model for Freeway Traffic Mixed with Connected Automated Vehicles and Regular Human-Piloted Vehicles." *Transportmetrica A: Transport Science* 1–29.

Park, M., K. Jang, J. Lee, and H. Yeo. 2015. "Logistic Regression Model for Discretionary Lane Changing Under Congested Traffic." *Transportmetrica A: Transport Science* 11 (4): 333–344.

Roncoli, C., M. Papageorgiou, and I. Papamichail. 2015. "Traffic Flow Optimisation in Presence of Vehicle Automation and Communication Systems–Part I: A First-Order Multi-Lane Model for Motorway Traffic." *Transportation Research Part C: Emerging Technologies* 57: 241–259.

Schakel, W. J., V. L. Knoop, and B. Van Arem. 2012. "Integrated Lane Change Model with Relaxation and Synchronization." *Transportation Research Record* 2316 (1): 47–57.

Seraj, M., Y. Bie, and T. Z. Qiu. 2017. "A Macroscopic Lane-changing Model for Freeway Considering Different Incentives and Traffic States." Paper presented at the 96th Annual Meeting of the Transportation Research Board.

Shiomi, Y., T. Taniguchi, N. Uno, H. Shimamoto, and T. Nakamura. 2015. "Multilane First-Order Traffic Flow Model with Endogenous Representation of Lane-Flow Equilibrium." *Transportation Research Part C: Emerging Technologies* 59: 198–215.

Toledo, T., H. Koutsopoulos, and M. Ben-Akiva. 2003. "Modeling Integrated Lane-Changing Behavior." *Transportation Research Record: Journal of the Transportation Research Board* 1857: 30–38.

Treiber, M., and D. Helbing. 2003. "Memory Effects in Microscopic Traffic Models and Wide Scattering in Flow-Density Data." *Physical Review E* 68 (4): 046119.

Treiber, M., and A. Kesting. 2013. *Traffic Flow Dynamics. Traffic Flow Dynamics: Data, Models and Simulation*. Berlin: Springer-Verlag.

Wang, J. 2005. "A Simulation Model for Motorway Merging Behaviour." *Transportation and Traffic Theory* 16: 281–301.

Wang, Y., and M. Papageorgiou. 2005. "Real-time Freeway Traffic State Estimation Based on Extended Kalman Filter: a General Approach." *Transportation Research Part B: Methodological* 39 (2): 141–167.

Wu, N. 2006. "Equilibrium of Lane Flow Distribution on Motorways." *Transportation Research Record* 1965 (1): 48–59.

Yuan, K., V. L. Knoop, L. Leclercq, and S. P. Hoogendoorn. 2017. "Capacity Drop: a Comparison Between Stop-and-go Wave and Standing Queue at Lane-Drop Bottleneck." *Transportmetrica B: Transport Dynamics* 5 (2): 145–158.

Zhang, H. M. 1999. "A Mathematical Theory of Traffic Hysteresis." *Transportation Research Part B: Methodological* 33 (1): 1–23.